ENVIRONMENTAL RESEARCH
LETTERS

LETTER • OPEN ACCESS

Holocene peat humification and carbon dynamics in the Westerlies-influenced Northwest China

IOP Publishing Environ. Res. Lett. 15 (2020) 124014 https://doi.org/10.1088/1748-9326/abc4fd

Environmental Research Letters

CrossMark

OPEN ACCESS

RECEIVED
30 May 2020

REVISED
10 October 2020

ACCEPTED FOR PUBLICATION
27 October 2020

PUBLISHED
24 December 2020

LETTER

Holocene peat humification and carbon dynamics in the Westerlies-influenced Northwest China

Yinbo Li, Liang Chen and Min Ran

College of Resource and Environmental Science, Xinjiang University, 666 Shengli Road, Urumqi 830046, People's Republic of China

E-mail: zhdl@ms.xjb.ac.cn **and** ran_anan@163.com

Keywords: peatland initiation, carbon accumulation, climate change, altai mountains, central asia

Supplementary material for this article is available online

Abstract

Understanding peat carbon dynamics in the past is of significance, given the uncertainties as to whether there will be an increase or a reduction in carbon as a result of future climate change. Studies of peat carbon dynamics have primarily been conducted in monsoon-influenced China. However, data relating to carbon dynamics in peat deposits has not yet been investigated in Westerlies-influenced Northwest China (NWC). In this study, the Holocene carbon accumulation rate (CAR) is explored at the Tuolehaite peat core, with a mean rate of growth of 2.4 yr mm^{-1}, 0.4 mm yr^{-1}, in the high-elevation Altai Mountains within NWC. Its CAR shows a decreasing trend, ranging from 4.8 to 68.8 g C m^{-2} yr^{-1}, with a mean of 28.0 g C m^{-2} yr^{-1} since the Holocene epoch. Comparisons of the CAR in the Westerlies-influenced NWC with that in the monsoon-influenced Qinghai-Tibetan Plateau, Northeast China, and South China, reveal that the Holocene CAR trend in relatively high-elevation peat deposits (e.g. Tuolehaite Peat and Hongyuan Peat) is opposite to that found in relatively low-elevation peat deposits (e.g. Hani Peat and Dahu Peat). Different driving factors (temperature and precipitation) of CAR could be responsible for these opposing trends. To be specific, temperature is the main driving factor influencing the CAR in relatively high-elevation peat deposits, whereas precipitation is the key driving factor controlling the CAR in relatively low-elevation peat deposits. Our work indicates that comprehensive investigations into peat CARs in both Westerlies-influenced and monsoon-influenced regions contribute to an understanding of the peat CAR pattern in China as a whole.

1. Introduction

Wetlands are a special type of ecosystem, occurring between the aquatic ecosystem and the terrestrial ecosystem, having the highest carbon density and the fastest carbon accumulation rate (CAR) (Liu *et al* 2006, Lv 2008). It covers only 6%–8% of the land area in the world, and its carbon storage has been estimated to be 500 ± 100 Pg C since the Last Glacial Maximum (Yu 2011). This is equivalent to approximately one-third of the total C pool on earth (Mitra *et al* 2005, Limpens *et al* 2008). The carbon accumulations of wetlands are dependent on the balance between primary production and decomposition, determined by temperature and precipitation (Charman 2002, Friedlingstein *et al* 2006, Cai *et al* 2010). In the context of global warming, the question of whether wetland will turn from carbon accumulation to carbon emission has attracted increased attention (Roulet *et al* 2007, Mcguire *et al* 2009, Oh *et al* 2020).

Large spatial-scale estimations of carbon dynamics have been performed in northern peatland, including western Siberia, Europe and North America (Vitt *et al* 2000, Yu 2009, Jones and Yu 2010, Yu *et al* 2010, Gorham *et al* 2012). The CAR from peat cores and their controlling factors have also been investigated in China (e.g. Wang *et al* 2014, Zhao *et al* 2014, Xing *et al* 2015, Zhang *et al* 2015, Wei *et al* 2018, Liu *et al* 2020). These studies all focus on monsoon-influenced regions, including the Qinghai-Tibetan Plateau (QTP), Northeast China (NEC) and South China (SC). There is little information in existing research relating to CAR variations and their controlling factors in the arid areas of Northwest China (NWC). The climate of arid NWC is dominated by the prevailing Westerlies, and is characterized by an increasing trend towards moisture during the Holocene epoch, in contrast to the Holocene moisture trend in monsoon-dominated regions (i.e. QTP, NEC and SC) (Chen *et al* 2008, Zhang and Feng 2018).

The purpose of our study is to perform high-resolution chronological analysis of Tuolehaite Peat in the Altai Mountains, in order to explore changes in CAR during the Holocene, and to detect its possible driving factors by comparing the information obtained with existing local and regional palaeoclimatic data. Our work attempts to (i) deepen our understanding of wetland ecosystems during the evolution of the Holocene westerlies, and (ii) provide valuable insights into carbon dynamics in the varied climatic regions of China.

2. Study area

The Altai Mountains are an important geographical division between the taiga forests and the steppe deserts (Chen *et al* 2008), and also represent important climatic conjunction between the Westerlies airflows and the Asian monsoonal airflows during the Holocene period (Blyakharchuk *et al* 2004, 2007, Rudaya *et al* 2009, Wang and Feng 2013, Feng *et al* 2017). The Altai Mountains within China (46°30′35″–49°10′45″N, 85°31′37″–91°01′15″E), in particular the southern slope of the middle Altai Mountains, are characterized by a ladder fault-block feature, and decreasing elevation in a northwest-southeast direction (Zhang *et al* 2016, Feng *et al* 2017). This mountainous belt has a very wet and cool environment, as compared with the arid climate in Central Asia (Chen *et al* 2008). The mean annual temperature is −3.6–1.8 °C. The coldest-month temperature in January is −14 °C, and the warmest-month temperature in July is <16 °C. The water vapor along the Irtysh valley is transported by the Westerlies, and precipitation has an obvious gradient of elevation: 200–300 mm, 300–500 mm, and 500–600 mm in low, middle and high elevations, respectively (Wang and Zhang 2019, Li *et al* 2020). The wetlands in the poorly-drained intermontane basins cover about 108 811.8 hm^2, distributed at elevations from 1700–2500 m a.s.l. (Nurbayev *et al* 2008). They are primary reservoirs of terrestrial carbon, and are particularly sensitive to climate change (Zhang *et al* 2016, Feng *et al* 2017, Zhang and Feng 2018, Xu *et al* 2019, Rao *et al* 2019, 2020, Yang *et al* 2019).

3. Material and methods

3.1. Study site and peat coring

The Tuolehaite Peat deposit (48.44°N, 87.54°E, 1700 m a.s.l.; site 1 in figure 1(a)), which developed in a small intermontane basin in the middle part of the southern Altai Mountains, is an ideal site for studying peat CAR changes, owing to its integrated and continuous deposits, and limited human disturbance. Modern vegetation around the peat is dominated by meadow steppe (see figure 1(b)), where *Carex pamirensis* and *Carex altai* represent the dominant plant life (figure 1(c)). A 380 cm sediment core was collected using a Holland peat corer (diameter 5 cm and length 50 cm) at Tuolehaite Peat in 2018. From these 50 cm cores, we collected samples of known volume every 2 cm over the whole peat sequence. The upper 358 cm of the core is composed of pure plant residues, and the lower 22 cm (i.e. 358–380 cm) is composed of clayey sediments (see figure 2).

3.2. Chronology

Eight peat samples were sent to the Beta Laboratory (Miami City, USA) for radiocarbon AMS dating, to establish the depth-age patterns of peat development. The selected samples without rootlets were deemed to be in an appropriate condition for radiocarbon analysis (see Table 1 in Zhang *et al* 2020a). Bacon age-modelling software (Blaauw and Christen 2011) is applied to establish a depth-age model, based on all ^{14}C dates (figure 2). This model simulates temporal deposition by assuming piece-wise linear accumulation, with accumulation rates, and the associated variability between nearby depths, constrained by prior information. The model is based on more than 5000 stored MCMC iterations, and has a stable run (right-first panel of figure 2). All settings are in their default mode, and the section thickness is set at 5 cm (right-third panel of figure 2). Based on the depth-age model, the Tuolehaite Peat core covers the past ∼10 650 cal. yr BP, with a clayey lacustrine layer occurring between ∼10 650 and ∼10 200 cal. yr BP (figure 2).

3.3. Dry bulk density and loss on ignition (LOI)

All samples were dried at 105 °C overnight, weighed, and then combusted in a muffle furnace at 550 °C for 4 h before being reweighed to determine dry bulk density and LOI (Dean 1974, Heiri *et al* 2001). The dry bulk density (g cm^{-3}) was calculated by dividing the dry peat weight (g) by the wet peat volume ($v = 1/2 \times \pi \times 2.5^2 \times 2 = 19.64$ cm^3). The total organic content (TOC) was estimated by multiplying the LOI by 0.5, based on previous Chinese data in (Yin *et al* 1991, Xin *et al* 2015). The LOI and dry bulk density analyses were performed at the Xinjiang Institute of Ecology and Geography, Chinese Academy of Sciences.

3.4. Humification analyses

Humification was analyzed via the commonly-used alkali-extraction method (Blackford and Chambers 1993). The measured value was expressed in terms of the percentage of light absorbance, which is proportional to the degree of peat humification (i.e. a lower value shows a lower degree of humification,

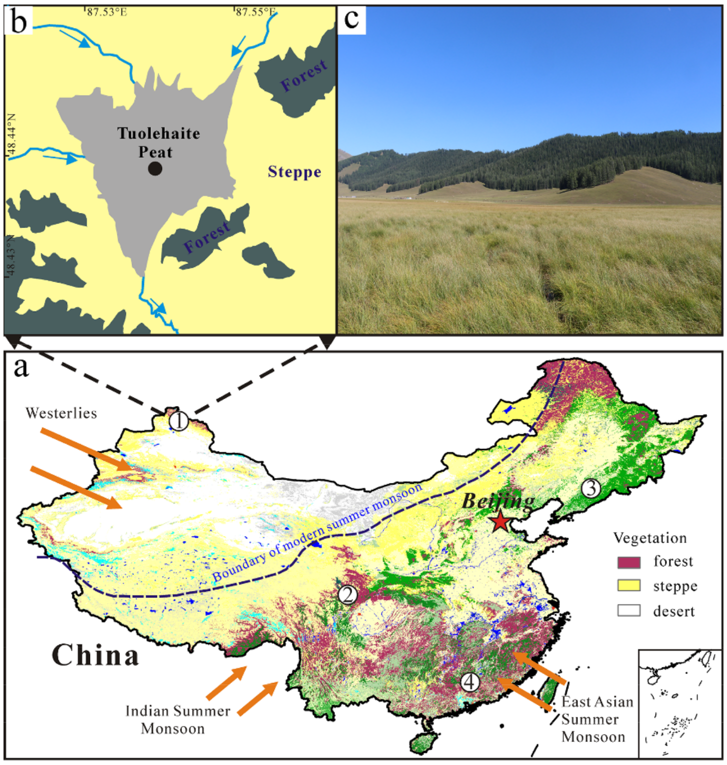

Figure 1. A: Location of Tuolehaite Peat (site 1) in China, together with other relevant sites (site 2, Hongyuan Peat; site 3, Hani Peat; site 4, Dahu Peat). Also included is a vegetation map of TLHT Peat and the surrounding area (b) including vegetation in and around the peat (c).

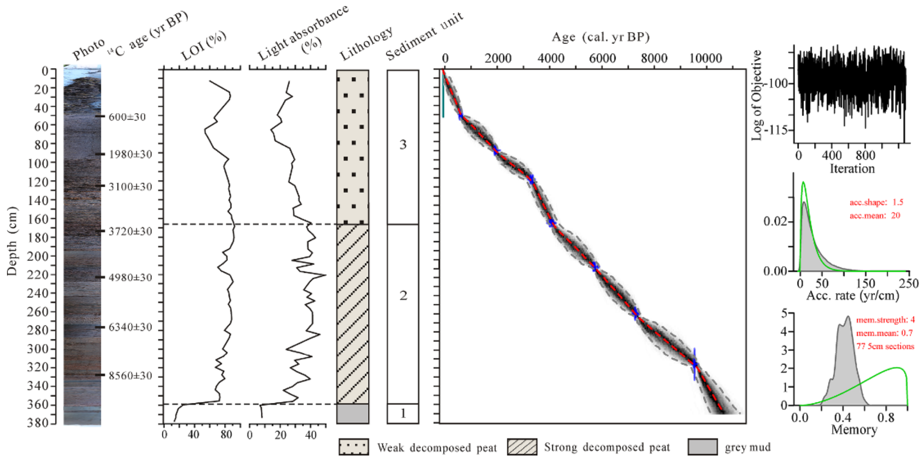

Figure 2. TLHT peat core: photo, dates, loss on ignition (LOI), light absorbance (%), lithology, sediment unit and depth-age model. Reprinted from Zhang *et al* 2020a, © 2020, with permission from Elsevier.
Note: chronological information may be found in Table 1 of Zhang *et al* (2020a).

and vice versa) (Aaby and Tauber 1975). The relationship between light absorbance and humification can be distorted by minerogenic constituents. It is therefore necessary to correct light absorbance values for any distortion caused by minerogenic constituents. A simple linear correction can be made based on the minerogenic content, as determined by LOI (Blackford and Chambers 1993, Chambers *et al* 2011, Zhang *et al* 2017). To remove aberrant data and 'random errors', the minerogenically-corrected humification data were smoothed via a 3-point moving-window smoothing method. In addition, humification has been proved to increase over time (Clymo 1984). To remove the time-dependency effect, the 3-point moving-window smoothed data for the humification sequence were detrended by applying a linear regression line (Newnham *et al* 2019), after which the residual values (i.e. the differences between the 3-point moving-window smoothed data and the linearly detrended data) can be considered as indicative of the degree of decomposition (Burrows *et al* 2014, Newnham *et al* 2019).

3.5. Peat growth and carbon accumulation rates

The peat growth rate (PGR; mm yr^{-1}) at Tuolehaite Peat was calculated based on the depth-age model and the thickness of the peat samples. The CAR was calculated via the following equation (Tolonen and Turunen 1996), based on raw data including PGR, dry bulk density, and TOC measurements:

$$\mathrm{CAR} = \mathrm{PGR}/1000 \times d \times c \tag{1}$$

where CAR is the carbon accumulation rate (g C m^{-2} yr^{-1}), PGR denotes the peat growth rate (mm yr^{-1}), d is the dry bulk density (g m^{-3}), and c is the TOC content (g C g^{-1} dry weight). The related data including dry bulk density, TOC, humification and carbon accumulation rates are provided in supplementary materials (stacks.iop.org/ERL/15/124014/mmedia).

4. Results

4.1. Development of the peat

In the stratigraphic profile of the Tuolehaite Peat (figure 2), three units were observed, based on sedimentary facies, LOI, and light absorbance (figure 2). Unit 1 (380–358 cm, ∼10 650 to ∼10 200 cal. yr BP) is a grayish lacustrine layer with low LOI (mean 20.50%) and light absorbance (mean 6.32%). Unit 2 (358–164 cm, ∼10 200 to ∼4010 cal. yr BP) is a strongly-decomposed peat layer with higher LOI (mean 81.23%) and light absorbance (mean 36.54%). Unit 3 (164–0 cm, ∼4010–0 cal. yr BP) is a poorly-decomposed peat layer with decreasing trends of LOI (mean 75.86%) and light absorbance (mean 25.70%). The combined distribution within the peat profile, in terms of bulk density (see figure 3(b)), indicates that the profile (358–2 cm, units 2 and 3) is representative of ombrotrophic peats (Shotyk 1996). The temporal changes in these properties show a strong, rapid transition to ombrotrophization, from the minerogenic phase beginning at ∼10 200 cal. yr BP, and is definitely established at a depth of 358 cm.

4.2. Humification, dry density and total organic carbon (TOC)

Having performed the minerogenical correction and the removal of the time-dependency-effect, humification (i.e. light absorbance) in the ombrotrophic phase experiences one lower-value interval, at ∼10 200 to ∼8200 cal. yr BP, one higher-value interval at ∼8200 to ∼4000 cal. yr BP, and then a decreasing trend at ∼4000 to ∼1200 cal. yr BP. There is an increasing trend in the past 1200 years (see figure 3(a)). The mean dry density (g cm^{-3}) at the Tuolehaite profile is 0.2 ± 0.1 g cm^{-3} (figure 3(b)). A clear decrease in dry density is observed towards the surface of the profile, with a value of 1.1 g cm^{-3} in the bottom layer (380 cm), and 0.1 g cm^{-3} in the surface layer (2 cm).

The mean TOC at the Tuolehaite profile is 39.2%, with a maximum value of 46.3% in the ombrotrophic phase, and a minimum value of 8.7% in the minerogenic phase (figure 3(c)). The TOC sequence can be classified into three stages in the ombrotrophic phase, i.e., since ∼10 200 cal. yr BP: high TOC at ∼10 200 to ∼7600 cal. yr BP, with a mean of 37.0%, higher TOC at ∼7600 to ∼3500 cal. yr BP, with a mean of 42.9%, and then a decreasing TOC, ranging from 43.9% to 30.1%, since ∼3500 cal. yr BP.

4.3. Peat growth rate (PGR) and carbon accumulation rates (CAR)

The mean PGR at Tuolehaite Peat is 0.4 mm yr^{-1} (2.4 yr mm^{-1}). The PGR sequence shows that the growth of peat has been continuous at variable rates (see figure 3(d)). Specifically, for the period prior to ∼9700 cal. yr BP, the PGR (0.5 mm yr^{-1}) was relatively high, and was followed by relatively low values, with a mean of 0.2 mm yr^{-1}, between ∼9700 and ∼7600 cal. yr BP. The PGR slightly increased (0.3 mm yr^{-1}) between ∼7600 and ∼4300 cal. yr BP, and then abruptly increased to a high level, with a mean of 0.6 mm yr^{-1}, at ∼4300 to ∼3500 cal. yr BP. The PGR decreased rapidly at ∼3500 cal. yr BP, dropping to 0.25 mm yr^{-1}, before switching to a high level (mean 0.7 mm yr^{-1}) in the past 1000 years.

The mean CAR is 28.0 ± 10.5 g C m^{-2} yr^{-1} at the Tuolehaite Peat core (figure 3(e)). During the initial period of peat formation (∼10 200 to ∼9700 cal. yr BP), the CAR (40.0 g C m^{-2} yr^{-1}) was higher than the mean value of the whole profile. In the following two millennia (∼9700 to ∼7500 cal. yr BP), the CAR (25.0 g C m^{-2} yr^{-1}) reduced. The CAR recovered between ∼7500 and ∼5800 cal. yr BP, followed by a decreasing trend between ∼5800 and ∼4200 cal. yr BP, with a mean of 23.7 g C m^{-2} yr^{-1}. The largest increase in CAR (40.1 g C m^{-2} yr^{-1}) throughout the entire Holocene was detected between ∼4200 and ∼3400 cal. yr BP. The CAR values in the past ∼3400 cal. yr BP showed a decreasing trend, with a mean of 18.4 g C m^{-2} yr^{-1}.

5. Discussions

5.1. Climate control in carbon accumulation

The mean CAR at Tuolehaite Peat was 28.0 g C m^{-2} yr^{-1} (figure 3(d)), which falls within the range reported by Borren *et al* (2004) (19–49 g C m^{-2} yr^{-1}) for western Siberia (located in the northern part of the Altai Mountains). It is largely lower than the CAR reported by Beilman *et al* (2009) for 77 peatland sites from western Siberia (42–88 g C m^{-2} yr^{-1}) and by Feurdean *et al* (2019) for Plotnikovo Mire, part of the Great Vaskugan Mire in western Siberia (35–90 g C m^{-2} yr^{-1}). Our mean CAR is similar to those of the boreal and subarctic peatlands in Canada (26.1 ± 3.6 g C m^{-2} yr^{-1}) (Garneau *et al* 2014), which is higher than the mean value

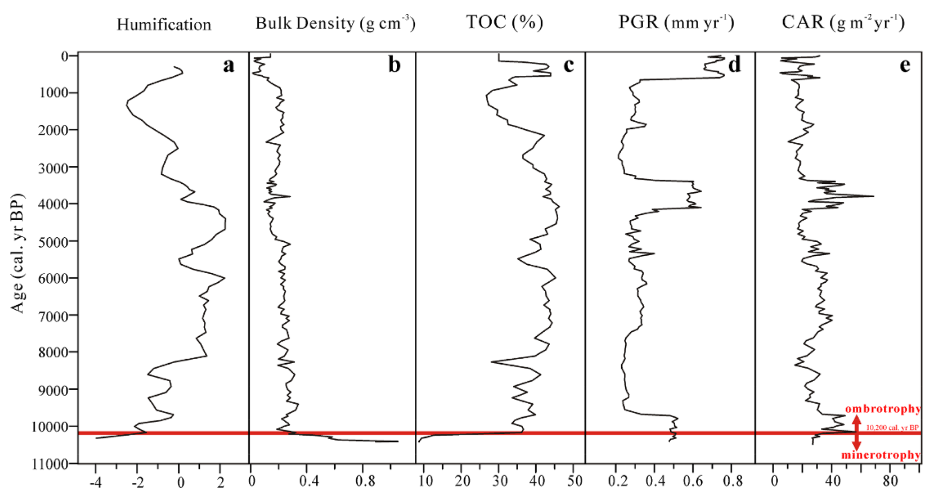

Figure 3. Properties of Tuolehaite Peat core (from a to e): humification, bulk density (BD, g cm^{-3}), total organic carbon (TOC), peat growth rate (PGR, mm yr^{-1}), and carbon accumulation rate (CAR, g m^{-2} yr^{-1}).
Note: humification data is inferred from minerogenically-corrected and time-dependency-effect-removed light absorbance values. Positive humification data indicates high peat decay, and negative humification data indicates low peat decay.

(23 ± 2 g C m^{-2} yr^{-1}) for northern peatlands (Loisel *et al* 2014). In China, the mean CAR (28.0 g C m^{-2} yr^{-1}) at Tuolehaite Peat is higher than that (26.4 g C m^{-2} yr^{-1}) found in the low-elevation Sanjiang Plain (including Hani Peat) (Xing *et al* 2015), and lower than that (34.9 g C m^{-2} yr^{-1}) found in the high-elevation Hengduan Mountains (including Hongyuan Peat) (Liu *et al* 2020) as well as (44.7 g C m^{-2} yr^{-1}) at the low-elevation Dahu Peat region in SC (Wei *et al* 2018).

The CAR of peat is primarily dependent on the balance between primary production and decomposition, which is generally modulated by temperature and precipitation (Svensson 1988, Laiho 2006). The CAR (4.8–68.8 g C m^{-2} yr^{-1}) at Tuolehaite Peat shows an overall decreasing trend since the Holocene era (figure 4(a)). The humification data indicates one high-decomposition interval at ~8200 to ~4000 cal. yr BP, and two low-decomposition intervals: at ~10 200 to ~8200, and since ~4000 cal. yr BP (figure 4(b)). The pollen A/C ratio-expressed moisture inferred from the same Tuolehaite core reveals a wet early Holocene (~10 600 to ~8500 cal. yr BP), a considerably dry middle Holocene (~8500 to ~4000 cal. yr BP), and a further wet period in the late Holocene (~4000–0 cal. yr BP) (figure 4(c)) (Zhang *et al* 2020a), with this analysis being supported by the recorded molecular markers, P_{aq} (the proportion of aquatic components), and moisture variations inferred from the nearby Ganhaizi Peat region (48°21′N, 87°41′E, 1926 m a.s.l.) (see figure 4(d)) based on unpublished data by Ran *et al*. The taiga biome score-indicated temperature inferred from data relating to the Kelashazi Peat region (48°07′N, 88°22′E, 2422 m a.s.l.) shows a warming early Holocene (before ~8200 cal. yr BP), a warmer middle Holocene (~8200 to ~4500 cal. yr BP), and a cooling late Holocene (since ~4500 cal. yr BP) (see figure 4(e)) (Wang and Zhang 2019, Zhang *et al* 2020b). This temperature trend is supported by the alkenone-recorded temperature variations recorded at Balikun Lake (43°36′N, 93°42′E, 580 m a.s.l.) in the nearby Tianshan Mountains (figure 4(f)) (Zhao *et al* 2017). Combined with these data regarding changes in peat humification, temperature and precipitation, other potential forcing factors relevant to Holocene carbon dynamics at Tuoleheite Peat are investigated below.

One of the phases of high CAR (40.0 g C m^{-2} yr^{-1}) occurs at the beginning of peat formation at Tuolehaite Peat (figure 4(a)), which coincides with the cold and wet climate at the beginning of the Holocene era (~10 200 to ~9700 cal. yr BP) (see figures 4(c)–(f)). The latter may result from the major forcing of the Laurentide ice sheet and other high-latitude ice sheets (Zhao *et al* 2017, Wang and Zhang 2019). These climatic conditions limited peat decay in this period (figure 5(b)), which was conducive to the preservation of peat plants, and a concomitant increase in CAR. In the following two millennia, i.e., from ~9700 to ~7500 cal. yr BP, the reduction in CAR (25.0 g C m^{-2} yr^{-1}) (figure 5(a)) coincides with a relatively cold and drying climate (figures 4(c)–(f)). Compared with the former interval (i.e., ~10 200 to ~9700 cal. yr BP), increasing humification could be responsible for the reduction in CAR during this period. A phase of notable recovery in CAR at ~7500 to ~5800 cal. yr BP corresponds well with the warmest and driest climatic conditions. The warmest climate may have led to the highest level of plant growth at Tuoleheite Peat. However, the warm-dry climate also contributes to a high level of decay in peat-living plants, due to increasing microbial activity in an aerobic environment; therefore, no

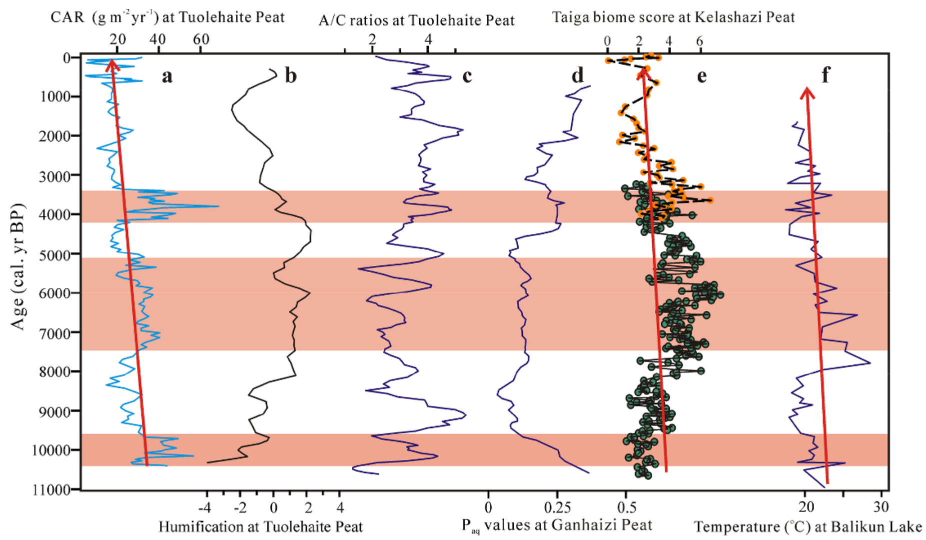

Figure 4. Investigations of driving factors of the carbon accumulation rate (CAR) at Tuolehaite Peat: a: CAR at Tuolehaite Peat (in this study); b: humification at Tuolehaite Peat (in this study); c: A/C ratio-expressed moisture at Tuolehaite Peat (Zhang *et al* 2020a); d: P_{aq}-expressed moisture at Ganhaizi Peat (Ran *et al* unpublished data); e: Taiga biome score at Kelashazi Peat (Wang and Zhang 2019, Zhang *et al* 2020b); f: Alkenone-recorded temperature at Balikun Lake (Zhao *et al* 2017).

higher CAR was observed during this interval (Zhang *et al* 2020a). The CAR once again fell below the mean CAR of the profile as a whole during the period from ~5800 to ~4200 cal. yr BP (figure 5(a)), which resulted from the combined effects of cold-dry climate, and high humification. Furthermore, the CAR exhibited a rapid increase at ~4200 to ~3400 cal. yr BP (figure 4(a)), which coincides with a marked decrease in humification, and a slightly wetter and warmer climatic conditions. These conditions may have contributed to the higher net primary productivity indicated by the higher TOC at Tuolehaite Peat (see figure 3(c)). The next significant drop in CAR at Tuolehaite Peat was identified in the period since ~3400 cal. yr BP, which coincides with a period of cold and wet climatic conditions.

Overall, the long-term trend of CAR at Tuolehaite Peat is parallel with the temperature trend during the Holocene interval. This indicates that the CAR in the southern Altai Mountains is primarily modulated by changes in temperature, and is also partly influenced by peat decomposition. A warming climate would enhance net primary productivity, owing to an increase in growing-season length in the Altai Mountains, and vice versa (Charman *et al* 2013).

5.2. Comparison with other peat carbon accumulations in China

As discussed above, studies of peat CAR in China mainly focus on monsoon-influenced regions, including QTP (Wang *et al* 2014, Zhao *et al* 2014, Liu *et al* 2020), NEC (Wang *et al* 2014, Zhao *et al* 2014, Xing *et al* 2015, Zhang *et al* 2015), and SN (Wei *et al* 2018). Climate changes in these regions are predominantly influenced by the Indian Summer Monsoon (ISM), and the East Asian Summer Monsoon (EASM) (Zhao *et al* 2009). In contrast, climate of the Altai Mountains in the arid NWC is primarily influenced by the prevailing Westerlies (Chen *et al* 2008, Wang and Feng 2013, Feng *et al* 2017, Zhang and Feng 2018). Investigations into CAR in the Westerlies-influenced NWC could provide valuable insights into the modulating factors of carbon dynamics in the different climatic regions of China. Here, we compare the Holocene CAR of Tuolehaite Peat (48.44°N, 87.54°E, 1700 m a.s.l.) in NWC with that gathered from three representative sites in monsoon-influenced regions (QTP, NEC and SC). Three representative sites are selected, including Hongyuan Peat in QTP (site 2 in figure 1(a), 32°46′N, 102°31′E, 3527 m a.s.l., Cai *et al* 2014), Hani Peat in NEC (site 3 in figure 1(a), 42°13′N, 126°31′E, 900 m a.s.l., Cai *et al* 2013), and Dahu Peat in SN (site 4 in figure 1(a), 24°45′N, 115°02′E, 246 m a.s.l., Wei *et al* 2018).

As shown in figure 5, the Tuolehaite CAR in NWC, ranging from 4.8 to 68.8 g C m^{-2} yr^{-1} (28.0 g C m^{-2} yr^{-1} on average) shows a decreasing trend since the Holocene period, with two episodes of higher CAR, prior to ~9600 cal. yr BP, and at ~4200 to ~3400 cal. yr BP (see figure 5(a)). In the QTP, the Hongyuan CAR ranges from 9.8 to 80.1 g C m^{-2} yr^{-1}, with a mean of 33.6 g C m^{-2} yr^{-1} (Cai *et al* 2014). The long-term CAR trend at Hongyuan Peat (figure 5(b)) is basically consistent with that at Tuolehaite Peat (figure 5(a)). The CAR inferred from Hani Peat in NEC ranges from 8.6 to 168.5 g C m^{-2} yr^{-1} (mean 41.2 g C m^{-2} yr^{-1}) (Cai *et al* 2013). During the Holocene, the Hani CAR can be defined in four stages: (1) a relatively low and stable CAR before ~8200 cal. yr BP; (2) a relatively high CAR between ~8200 and ~4000 cal. yr BP; (3) a further period of decreasing CAR between ~4000 and ~1500 cal. yr BP; and (4) rapidly increasing CAR in the past 1500 years

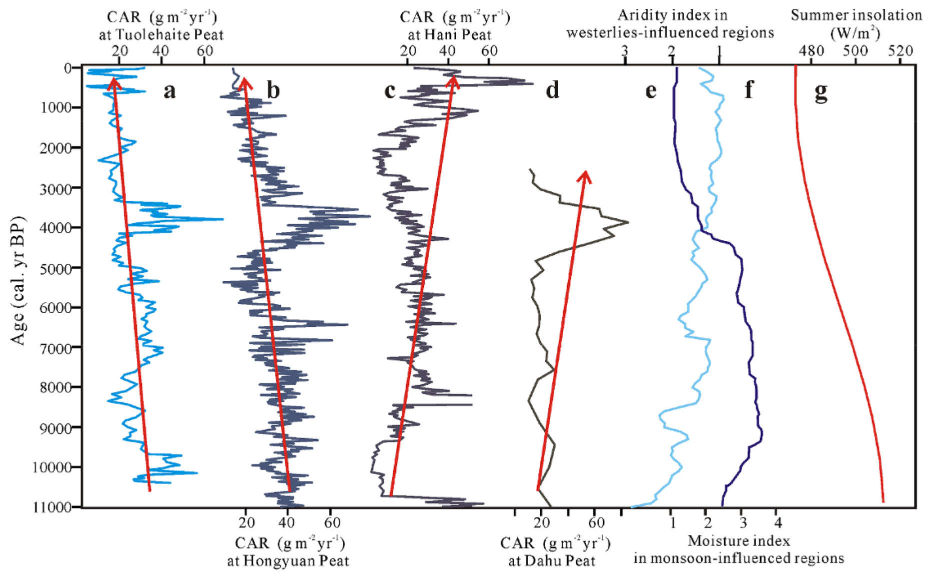

Figure 5. Comparison of carbon accumulation rate (CAR) for Tuolehaite Peat with those for Hongyuan Peat, Hani Peat, Dahu Peat, and other palaeoclimatic records of the Holocene interval. a: CAR at Tuolehaite Peat (in this study); b: CAR at Hongyuan Peat (Cai *et al* 2013); c: CAR at Hani Peat (Cai *et al* 2014); d: CAR at Dahu Peat (Wei *et al* 2018); e: moisture index in the monsoon-influenced regions (Zhao *et al* 2009); f: aridity index in the Westerlies-influenced regions (Zhang and Feng 2018); g: summer insolation (Berger and M F 1991).

(figure 5(c)) (Cai *et al* 2013). The CAR (19.7–85.2 g C m^{-2} yr^{-1}) at Dahu Peat in SC shows a low and stable level prior to ~4500 cal. yr BP, and an abruptly increasing trend since ~4500 cal. yr BP (figure 5(d)) (Wei *et al* 2018).

Comparisons of CAR in the different climatic regions of China (NWC, QTP, EC and SC) reveal that the Holocene CAR in the EASM-influenced Hani Peat and Dahu Peat shows an inverse trend as compared with that of the ISM-influenced Hongyuan Peat, and the Westerlies-influenced Tuolehaite Peat (figures 5(a)–(d)). Differences in the driving factors of peat development may be responsible for this inverse trend. Specifically, Hani Peat and other sites in NEC (15 sites in Zhang *et al* 2015; 43 sites in Xing *et al* 2015) and Dahu Peat were sampled from shallow basins or lakes. A rather warm and wet climate dominated in the monsoonal regions during the early Holocene (figure 5(e)) (Wang *et al* 2005, Zhao *et al* 2009), which favoured the incidence of widespread lacustrine deposits with low organic carbon content in shallow basins, and produced a low CAR in NEC and SC (Xing *et al* 2015, Zhang *et al* 2015, Wei *et al* 2018). In the past ~4200 cal. yr BP, a weakening EASM and the related drying climate (figure 5(e)) has led to the accumulation of organic-carbon-rich sediments (i.e. higher CAR) in NEC and SC (figures 5(c)–(d)). Therefore, we propose that precipitation could be an important factor modulating the CAR in peat regions in NEC and SC. It should be noted that the increasing CAR at Hani Peat during the past 1500 years (figure 5(c)) is attributable to the rising moisture in the context of a cooling climate in NEC (Cai *et al* 2013).

Conversely, high summer insolation and strong climate seasonality (figure 5(g)) in the early-middle Holocene (Zhao and Z C 2012, Zhao *et al* 2014) resulted in higher CAR at the high-elevation Tuolehaite Peat in NWC (figure 5(a)) and at Hongyuan Peat in QTP (figure 5(b)). An increased temperature would enhance primary productivity, due to the extension of the growing season of plants in these relatively high-elevation regions (Charman *et al* 2013, Zhao *et al* 2014). The warm climate could also improve peat decay by stimulating microbial activity (Ise *et al* 2008, Dorrepaal *et al* 2009). However, the decomposition process may only have a minor effect on primary productivity at high-elevation regions in QTP and NWC, due to strong seasonality at higher elevations, with increasing plant production in short-warm summers, and the cessation of peat decomposition in long, cold winters (Wei *et al* 2018). Subsequent decreases in CAR in QTP and NWC during the middle and late Holocene are attributable to the subsequent summer-insolation-induced cooling climate (figure 5(g)) (Berger and M F 1991). The decreasing trends in CAR in the high-elevation areas of QTP and NWC are consistent with the northern peatland CAR variations during the Holocene (Yu *et al* 2010). Huang *et al* (2018) and Zhang *et al* (2020b) confirm that vegetation changes in the high-elevation Altai Mountains are modulated by the insolation-driven temperature change in the context of a wetter Holocene trend (figure 5(f)) (Zhang and Feng 2018). A similar vegetation-climate relationship in QTP has previously been reported by Zhao *et al* (2009). We therefore propose that temperature is a key factor influencing peat CAR in relatively high-elevation peat deposits (e.g. Hongyuan Peat and Tuolehaite Peat), while precipitation is the key factor controlling the CAR in relatively low-elevation peat deposits (e.g. Hani Peat and Dahu Peat).

6. Conclusions

In this paper, we have investigated the carbon accumulation rates (CAR) at Tuolehaite Peat in the Westerlies-influenced Altai Mountains in NWC. The results indicate that the CAR at Tuolehaite Peat experienced a decreasing trend, with a mean of 28.0 g C m^{-2} yr^{-1}, during the Holocene interval. Compared with the CAR trend in the monsoon-influenced QTP, NEC and SC, the Holocene CAR trends at Tuolehaite Peat in the Altai Mountains, and at Hongyuan Peat in the QTP, are opposite to those found at Hani Peat in NEC and at Dahu Peat in SC. These opposing trends in relation to CAR appear to result from specific influencing factors (i.e., temperature and precipitation) at relatively high and low elevations.

Acknowledgments

This research was financially supported by the Postdoctoral Science Foundation of China (No. 2019M663864), the National Natural Science Grants of China (No. 41803024 and 41502168), the Postdoctoral Innovative Talent Support Program of China (No. BX20190363), and the Western Young Scholar Program-B of Chinese Academy of Sciences (2018-XBQNXZ-B-020). We appreciate editors for improving the English writing, and we thank two anonymous reviewers for their valuable comments and constructive suggestions.

Data availability statement

All data supporting the findings of this study are included within the article (and any supplementary information files).

References

Aaby B and Taube H 1975 Rates of peat formation in relation to degree of humification and local environment, as shown by studies of a raised bog in Denmark *Boreas* **4** 1–17

Beilman D W *et al* 2009 Carbon accumulation in peatlands of West Siberia over the last 2000 years *Glob. Biogeochem. Cycles* **23 GB** 1012

Berger A and Loutre M F 1991 Insolation values for the climate of the last 10 million years *Quat. Sci. Rev.* **10** 297–317

Blackford J J and Chambers F M 1993 Determining the degree of peat decomposition for peat-based palaeoclimate studies *Int. Peat J.* **5** 7–24

Blaauw M and Christen J A 2011 Flexible paleoclimate age-depth models using an autoregressive gamma process *Bayesian Anal.* **6** 457–74

Blyakharchuk T A, Wright H E, Borodavko P S, van der Knaap W O and Ammann B 2004 Late glacial and Holocene vegetation changes on the Ulagan high-mountains plateau, Altai Mountains, southern Siberia *Palaeogeogr. Palaeoclimatol. Palaeoecol.* **209** 259–79

Blyakharchuk T A, Wright H E, Borodavko P S, Van der Knaap W O and Ammann B 2007 Late Glacial and Holocene vegetational history of the Altai Mountains (southwestern Tuva Republic, Siberia) *Palaeogeogr. Palaeoclimatol. Palaeoecol.* **245** 518–34

Borren W, Bleuten W and Lapshina E D 2004 Holocene peat and carbon accumulation rates in the southern taiga of western Siberia *Quat. Res.* **61** 42–51

Burrows M A, Fenner J and Haberle S G 2014 Humification in northeast Australia: dating millennial and centennial scale climate variability in the late Holocene *Holocene* **24** 1707–18

Cai C *et al* 2013 Holocene peat carbon accumulation rates and influence factors from the Hani peatland, Northeast China *Earth Environ.* **41** 597–604 in Chinese

Cai C *et al* 2014 Carbon accumulation rates and its influence factors in the Hongyuan Peat, Southwest China *Bull. Mineral. Petrol. Geochem.* **3** 309–16 in Chinese

Cai T, Flanagan L B and Syed K H 2010 Warmer and drier conditions stimulate respiration more than photosynthesis in a boreal peatland ecosystem: analysis of automatic chambers and eddy covariance measurements *Plant Cell. Environ.* **33** 394–407

Chambers F M *et al* 2011 Methods for determining peat humification and for quantifying peat bulk density, organic matter and carbon content for palaeostudies of climate and peatland carbon dynamics *Mires Peat* **7** 1–10

Charman D 2002 *Peatlands and Environmental Change* (New York: Wiley)

Charman D *et al* 2013 Climate-related changes in peatland carbon accumulation during the last millennium *Biogeosciences* **10** 1–16

Chen F H *et al* 2008 Holocene moisture evolution in arid central Asia and its out-of-phase relationship with Asian monsoon history *Quat. Sci. Rev.* **27** 351–64

Chen F H, Jia J, Chen J H, Li G Q, Zhang X S, Xie H C, Xia D S, Huang W and An C B 2016 A persistent Holocene wetting trend in arid central Asia, with wettest conditions in the late Holocene, revealed by multi-proxy analyses of loess-paleosol sequences in Xinjiang, China *Quat. Sci. Rev* **146** 134–46

Clymo R S 1984 The limits to peat bog growth *Phil. Trans. Roy. Soc. Lond.* B **303** 605–54

Dean W 1974 Determination of carbonate and organic matter in calcareous sediments and sedimentary rocks by loss on ignition: comparison with other methods *J. Sediment. Res.* **44** 242–8

Dorrepaal E, Toet S, van Logtestijn R S P, Swart E, van de Weg M J, Callaghan T V and Aerts R 2009 Carbon respiration from subsurface peat accelerated by climate warming in the subarctic *Nature* **460** 616–9

Feng Z D, Sun A Z, Abdusalih N, Ran M, Kurban A, Lan B, Zhang D L and Yang Y P 2017 Vegetation changes and associated climatic changes in the southern Altai Mountains within China during the Holocene *Holocene* **27** 683–93

Feurdean A, Gałka M, Florescu G, Diaconu A-C, Tanţău I, Kirpotin S and Hutchinson S M 2019 2000 years of variability in hydroclimate and carbon accumulation in western Siberia and the relationship with large scale atmospheric circulation: a multiproxy peat record *Quat. Sci. Rev.* **226** 105948

Friedlingstein P *et al* 2006 Climate-carbon cycle feedback analysis: results from the C4MIP model intercomparison *J. Clim.* **19** 3337–53

Garneau M, van Bellen S, Magnan G, Beaulieu-Audy V, Lamarre A and Asnong H 2014 Holocene carbon dynamics of boreal and subarctic peatlands from Quebec, Canada *Holocene* **24** 1043–53

Gorham E, Lehman C, Dyke A, Clymo D and Janssens J 2012 Long-term carbon sequestration in North American peatlands *Quat. Sci. Rev.* **58** 77–82

Heiri O, Lotter A F and Lemcke G 2001 Loss on ignition as a method for estimating organic and carbonate content in sediments: reproducibility and comparability of results *J. Paleolimnol.* **25** 101–10

Huang X Z *et al* 2018 Holocene vegetation and climate dynamics in the Altai Mountains and surrounding areas *Geophys. Res. Lett.* **45** 6628–36

Ise T, Dunn A L, Wofsy S C and Moorcroft P R 2008 High sensitivity of peat decomposition to climate change through watertable feedback *Nat. Geosci.* **1** 763–6

Jones M C and Yu Z C 2010 Rapid deglacial and early Holocene expansion of peatlands in Alaska *PNAS* **107** 7347–52

Laiho R 2006 Decomposition in peatlands: reconciling seemingly contrasting results on the impacts of lowered water levels *Soil Biol. Biochemistry* **38** 2011–24

Li Y B *et al* 2020 Temporal-spatial variability of modern climate in the Altai Mountains during 1970–2015 *PloS One* **15** e0230196

Limpens J, Berendse F, Blodau C, Canadell J G, Freeman C, Holden J, Roulet N, Rydin H and Schaepman-Strub G 2008 Peatlands and the carbon cycle: from local processes to global implications-a synthesis *Biogeosci* **5** 1379–419

Liu L *et al* 2020 Peatland Development and Carbon Dynamics since the Last Glacial Maximum in the Hengduan Mountains Region *Catena* **190** 104525

Liu X T *et al* 2006 *Introduction to Swamp Science* Changchun: Jilin Science and Technology Press

Loisel J *et al* 2014 A database and synthesis of northern peatland soil properties and Holocene carbon and nitrogen accumulation *Holocene* **24** 1028–42

Lv X G 2008 *Wetland and wetland research in China* Shijiangzhuang: Hebei Science and Technology Press

Mcguire A D, Anderson L G, Christensen T R, Dallimore S, Guo L, Hayes D J, Heimann M, Lorenson T D, Macdonald R W and Roulet N 2009 Sensitivity of the carbon cycle in the Arctic to climate change *Ecol. Monogr.* **79** 523–55

Mitra S *et al* 2005 An appraisal of global wetland area and its organic carbon stock *Curr. Sci.* **88** 25–35

Newnham R M, Hazell Z J, Charman D J, Lowe D J, Rees A B H, Amesbury M J, Roland T P, Gehrels M, van den Bos V and Jara I A 2019 Peat humification records from Restionaceae bogs in northern New Zealand as potential indicators of Holocene precipitation, seasonality, and ENSO *Quat. Sci. Rev* **218** 378–94

Nurbayev A *et al* 2008 Peanlands of the Chinese Altay *Peatlands Int.* **2** 25–28

Oh Y *et al* 2020 Reduced net methane emissions due to microbial methane oxidation in a warmer Arctic *Nat. Clim. Change* **10** 321–7

Pontevedra-Pomba X, Castro D, Souto M, Fraga I, Blake W H, Blaauw M, López-Sáez J A, Pérez-Díaz S, Valcárcel M and García-Rodeja E 2019 10,000 years of climate control over carbon accumulation in an Iberian bog (southwestern Europe) *Geosci. Front.* **10** 1521–33

Rao Z G, Huang C, Xie L, Shi F, Zhao Y, Cao J, Gou X, Chen J and Chen F 2019 Long-term summer warming trend during the Holocene in Central Asia indicated by alpine peat α-cellulose δ^{13}C record *Quat. Sci. Rev.* **203** 56–67

Rao Z G, Shi F, Li Y, Huang C, Zhang X, Yang W, Liu L, Zhang X and Wu Y 2020 Long-term winter/summer warming trends during the Holocene revealed by α-cellulose δ^{18}O/δ^{13}C records from an alpine peat core from central Asia *Quat. Sci. Rev.* **232** 106217

Roulet N T, Lafleur P M, Richard P I E R R E J H, Moore T R, Humphreys E R and Bubier J 2007 Contemporary carbon balance and late Holocene carbon accumulation in a northern peatland *Global Change Biol.* **13** 397–411

Rudaya N, Tarasov P, Dorofeyuk N, Solovieva N, Kalugin I, Andreev A, Daryin A, Diekmann B, Riedel F and Tserendash N 2009 Holocene environments and climate in the Mongolian Altai reconstructed from the Hoton-Nur pollen and diatom records: a step towards better understanding climate dynamics in Central Asia *Quat. Sci. Rev.* **28** 540–54

Shotyk W 1996 Peat bog archives of atmospheric metal deposition: geochemical evaluation of peat profiles, natural variations in metal concentrations, and metal enrichment factors *Environ. Rev.* **4** 149–83

Svensson G 1988 Bog development and environmental conditions as shown by the stratigraphy of Store Mosse mire in southern Sweden *Boreas* **17** 89–111

Tolonen K and Turunen J 1996 Accumulation rates of carbon in mires in Finland and implications for climate change *Holocene* **6** 171–8

Vitt D H, Halsey L A, Bauer I E and Campbell C 2000 Spatial and temporal trends in carbon storage of peatlands of continental western Canada through the Holocene *Canadian J. Earth Sci.* **37** 683–93

Wang M *et al* 2014 Carbon dynamics of peatlands in China during the Holocene *Quat. Sci. Rev.* **99** 34–41

Wang W and Feng Z D 2013 Holocene moisture evolution across the Mongolian Plateau and its surrounding areas: A synthesis of climatic records *Earth-Sci. Rev.* **122** 38–57

Wang W and Zhang D L 2019 Holocene vegetation evolution and climatic dynamics inferred from an ombrotrophic peat sequence in the southern Altai Mountains within China *Global Planet. Change* **179** 10–22

Wang Y J *et al* 2005 The Holocene Asian monsoon: link to solar changes and North Atlantic climate *Science* **308** 854–7

Wei Z Q, Zhong W, Shang S, Xue J, Ouyang J, Zhu C, Tian L, Chen Y and Chen B 2018 Carbon accumulation in Dahu Swamp in the eastern Nanling Mountains (south China) and its implications for hydroclimatic variability over the past 47000 years *Boreas* **47** 469–80

Xing W, Bao K, Gallego-Sala A V, Charman D J, Zhang Z, Gao C, Lu X and Wang G 2015 Climate controls on carbon accumulation in peatlands of Northeast China *Quat. Sci. Rev.* **115** 78–88

Xu H, Zhou K E, Lan J H, Zhang G L and Zhou X Y 2019 Arid Central Asia saw mid-Holocene drought *Geology* **47** 255–8

Yang Y P, Zhang D L, Sun A Z, Wang W, Lan B and Feng Z D 2019 Pollen-based reconstructions of vegetation and climate changes during the late Holocene in the southern Altai Mountains *Holocene* **29** 1450–8

Yin S *et al* 1991 Peat Resource and its Exploitation and Utilization in China Beijing:Geological Press in Chinese

Yu Z C 2011 Holocene carbon flux histories of the world's peatlands: global carboncycle implications *Holocene* **21** 761–74

Yu Z C 2009 Sensitivity of northern peatland carbon dynamics to Holocene climate change *Carbon Cycling in Northern Peatlands Geophysical Monograph* ed A J Baird, L R Belyea, X Comas, A S Reeve and L D Slater *et al* vol *184* (Washington, DC: American Geophysical Union) pp 55–69

Yu Z C, Loisel J, Brosseau D P, Beilman D W and Hunt S J 2010 Global peatland dynamics since the last glacial maximum *Geophys. Res. Lett.* **37** L13402

Zhang D L *et al* 2017 Peat humification- and $\delta^{13}C_{cellulose}$-recorded warm-season moisture variations during the past 500 years in the southern Altai Mountains within northern Xinjiang of China *J. Mt. Sci.* **14** 2200–11

Zhang D L, Chen X, Li Y M, Ran M, Yang Y P, Zhang S R and Feng Z D 2020a Holocene moisture variations in the Arid Central Asia: new evidence from the southern Altai Mountains of China *Sci. Total Environ.* **735** 139545

Zhang D L, Chen X, Li Y M, Wang W, Sun A Z, Yang Y P, Ran M and Feng Z D 2020c Response of vegetation to Holocene evolution of westerlies in the Asian Central Arid Zone *Quat. Sci. Rev* **229** 106138

Zhang D L, Chen X, Li Y M and Zhang S R 2020b Holocene vegetation dynamics of the Altai Mountains in the Arid Central Asia *Palaeogeogr. Palaeoclimatol. Palaeoecol.* **550** 109744

Zhang D L and Feng Z D 2018 Holocene climate variations in the Altai Mountains and the surrounding areas: a synthesis of pollen records *Earth-Sci. Rev.* **185** 847–69

Zhang D L, Feng Z D, Yang Y P, Lan B, Ran M and Mu G J 2018 Peat $\delta^{13}C_{cellulose}$-recorded wetting trend during the past 8000 years in the southern Altai Mountains, northern Xinjiang, NW China *J. Asian Earth Sci.* **156** 174–9

Zhang Y, Meyers P A, Liu X T, Wang G P, Ma X H, Li X Y, Yuan Y X and Wen B L 2016 Holocene climate changes in the central Asia mountain region inferred from a peat sequence from Altai mountains, Xinjiang, northwestern China *Quat. Sci. Rev.* **152** 19–30

Zhang Z Q *et al* 2015 The peatlands developing history in the Sanjiang Plain, NE China, and its response to East Asian monsoon variation *Sci. Rep.* **5** 1–10

Zhao J J, An C B, Huang Y, Morrill C and Chen F H 2017 Contrasting early Holocene temperature variations between monsoonal East Asia and westerly dominated Central Asia *Quat. Sci. Rev.* **178** 14–23

Zhao Y *et al* 2014 Peatland initiation and carbon accumulation in China over the last 50 000 years *Earth-Sci. Rev.* **128** 139–46

Zhao Y and Yu Z C 2012 Vegetation response to Holocene climate change in East Asian monsoon- margin region *Earth-Sci. Rev.* **113** 1–10

Zhao Y, Yu Z C, Chen F H, Zhang J W and Yang B 2009 Vegetation response to Holocene climate change in monsoon-influenced region of China *Earth-Sci. Rev.* **97** 242–56